Glutamate Slows Axonal Transport of Neurofilaments in Transfected Neurons

Steven Ackerley,*‡ Andrew J. Grierson,*‡ Janet Brownlees,*‡ Paul Thornhill,*‡ Brian H. Anderton,* P. Nigel Leigh,‡ Christopher E. Shaw,‡ and Christopher C.J. Miller*‡

*Department of Neuroscience, ‡Department of Neurology, The Institute of Psychiatry, Kings College London, London SE5 8AF United Kingdom

Abstract. Neurofilaments are transported through axons by slow axonal transport. Abnormal accumulations of neurofilaments are seen in several neurodegenerative diseases, and this suggests that neurofilament transport is defective. Excitotoxic mechanisms involving glutamate are believed to be part of the pathogenic process in some neurodegenerative diseases, but there is currently little evidence to link glutamate with neurofilament transport. We have used a novel technique involving transfection of the green fluorescent protein–tagged neurofilament middle chain to measure neurofilament transport in cultured neurons. Treatment of the cells with glutamate induces a slowing of neurofilament transport. Phosphorylation of the side-arm domains of neurofilaments has been associated with a slowing of neurofilament transport, and we show that glutamate causes increased phosphorylation of these domains in cell bodies. We also show that glutamate activates members of the mitogen-activated protein kinase family, and that these kinases will phosphorylate neurofilament side-arm domains. These results provide a molecular framework to link glutamate excitotoxicity with neurofilament accumulation seen in some neurodegenerative diseases.

Key words: neurofilament proteins • phosphorylation • amyotrophic lateral sclerosis • Alzheimer's disease

Introduction

Neurofilaments are the major intermediate filaments of neurons and, in mature neurons, comprise three subunit proteins: neurofilament light chain (NF-L),[1] neurofilament middle chain (NF-M), and neurofilament heavy chain (NF-H; for review see Lee and Cleveland, 1996). Neurofilament proteins are synthesized in cell bodies and transported into and through axons, with other components of the cytoskeleton, by slow axonal transport. Neurofilament and microtubule proteins travel in slow component a, whereas actin and a number of other proteins travel in slow component b (for reviews see Baas and Brown, 1997; Hirokawa et al., 1997; Nixon, 1998). The speed of transport of neurofilaments varies between ~0.25 and 3 mm/d, and is dependent on a number of factors, including the type of neuron, location of neurofilament protein within the axon, and the age of the animal (Baas and Brown, 1997; Hirokawa et al., 1997; Nixon, 1998).

Accumulations of neurofilament proteins are seen in a number of neurodegenerative diseases. These include amyotrophic lateral sclerosis (ALS), Parkinson's disease, dementia with Lewy bodies, and Alzheimer's disease (Hirano, 1991; Trojanowski et al., 1993; Schmidt et al., 1996). Although it is not clear how neurofilament accumulations contribute to the neurodegenerative process in these diseases, their presence suggests that neurofilament transport is somehow disrupted in affected neurons. Indeed, direct measurements of axonal transport in several transgenic mouse models of ALS have revealed that slowing of neurofilament transport is a common and early pathological feature (Collard et al., 1995; Zhang et al., 1997; Williamson and Cleveland, 1999).

The events that might lead to the slowing of neurofilament transport are not known, but a body of evidence implicates excitotoxic mechanisms involving glutamate in several neurodegenerative diseases (Rothstein, 1996; Guo et al., 1999). However, there is currently no direct evidence to link excessive extracellular glutamate with the

Address correspondence to Christopher C.J. Miller, Department of Neuroscience, The Institute of Psychiatry, Denmark Hill, London SE5 8AF UK. Tel.: 2-07-848-0393. Fax. 2-07-708-0017. E-mail: chris.miller@iop.kcl.ac.uk

S. Ackerley and A.J. Grierson contributed equally to this work.

[1]*Abbreviations used in this paper:* ALS, amyotrophic lateral sclerosis; cdk5, cyclin-dependent kinase 5; EGFP, enhanced green fluorescent protein; GST, glutathione-S-transferase; MAPK, mitogen-activated protein kinase; MPR, multiphosphorylation repeat; NF-H, neurofilament heavy chain; NF-L, neurofilament light chain; NF-M, neurofilament middle chain; SAPK, stress-activated protein kinase.

slowing of neurofilament transport. Here, we have expressed enhanced green fluorescent protein–tagged NF-M (EGFP-NF-M) in cultured cortical neurons and show that it is transported through neurites at rates consistent with that of slow axonal transport. Transport of EGFP-NF-M is via a process that requires metabolic energy. We also demonstrate that treatment of the neurons with glutamate slows the velocity of EGFP-NF-M transport.

Materials and Methods

Cell Culture

Intermediate filament negative SW13− cells were grown in DME containing 10% (vol/vol) FBS supplemented with 2 mM glutamine, 100 IU/ml penicillin, and 100 μg/ml streptomycin (GIBCO BRL). Primary cortical neurons were obtained from E18 rat embryos and cultured on glass coverslips coated with poly-D-lysine and laminin in 12-well plates (Falcon) in neurobasal medium and B27 supplement (GIBCO BRL) containing 100 IU/ml penicillin, 100 μg/ml streptomycin, and 2 mM glutamine. Cells were cultured for 7 d and, under these conditions, were almost exclusively neurons (staining with antibodies to neurofilaments and glial fibrillary acidic protein) (Dako) revealed that glial cells comprised <0.1% of the population).

Plasmids and Cell Transfection

For expression of NF-L, NF-M, and NF-H, the rat cDNAs (Chin and Liem, 1989, 1990) were cloned as EcoRI fragments into pCIneo (Promega). NH_2-terminal EGFP-tagged rat NF-M was expressed by cloning a rat NF-M cDNA into the EcoRI site of pEGFP-C3 (CLONTECH) and β-galactosidase by cloning into pQBIAdCMV (Quantum) following end repair of both insert and vector.

7-d-old primary cortical neurons were transfected by calcium phosphate methods using a calcium phosphate Profection kit (Promega) essentially as previously described (Nikolic et al., 1996; Xia et al., 1996). In brief, neurons grown on coverslips in 12-well plates were transfected with 6 μg of pEGFP-NF-M plasmid DNA prepared using an EndoFree plasmid kit (Qiagen). As described previously (Xia et al., 1996), the duration of incubation with the DNA/calcium phosphate precipitate was dictated by how fast the precipitate formed on the plate that was routinely between 10 and 20 min. The incubation was stopped 20 min later by removal of the media and shocking with 2% DMSO/5% glycerol in Hepes-buffered saline. The cells were washed three times in culture media and returned to the incubator. The efficiency of transfection was routinely 1–3%, and since contaminating glial cells represent <0.1% of the cells in the population, the majority of transfected cells are neurons which is in agreement with earlier studies on cortical neurons using this transfection method (Nikolic et al., 1996; Xia et al., 1996). However, some coverslips were additionally immunostained for neurofilament proteins (see below) or glial fibrillary acidic protein to further demonstrate that transfected cells were neurons. SW13− cells were transfected as previously described using a calcium phosphate Profection kit (Gibb et al., 1996).

Immunofluorescence Studies and Detection of EGFP-NF-M

For immunofluorescence studies of both SW13− cells and neurons, cells were fixed in 4% (wt/vol) paraformaldehyde in PBS for 20 min, permeabilized in 0.1% (wt/vol) Triton X-100 in PBS for 10 min, blocked with 5% (vol/vol) FBS/0.2% (wt/vol) Tween 20 in PBS for 1 h, and probed with primary antibodies diluted in blocking solution. NF-L, NF-M, and NF-H were detected using antibodies NR4 (Sigma Chemical Co.), a polyclonal rabbit antibody to NF-L, NN18 (Roche), SMI36, and SMI32 (Affiniti). β-Galactosidase was detected using a rabbit polyclonal antibody (5′-3′ Inc.). Active p42 and p44 mitogen-activated protein kinases (p42/p44-MAPKs) and active stress–activated protein kinase (SAPK) were detected using antibodies that recognize the active forms of these kinases (Promega). Blocking solution for the active p42/p44MAPK and SAPK antibodies comprised 0.2% Tween 20 in TBS. Primary antibodies were detected using goat anti–mouse or goat anti–rabbit Igs coupled to Oregon green or Texas red (Molecular Probes), and the samples were mounted in Vectashield (Vector labs).

For studies of transfected EGFP-NF-M in primary cortical neurons, cells were fixed in 4% (wt/vol) paraformaldehyde in PBS, processed as above, and mounted in Vectashield. Transfected neurons were routinely stained with Hoechst 33258 (Molecular Probes) for analyses of nuclear morphology and fragmentation so as to assess any potential toxicity. Additionally, lactate dehydrogenase cell viability assays (CytoTox 96; Promega) were utilized to determine toxicity including that induced by glutamate. All cells were examined using a Zeiss Axioskop microscope, and images were collected via a CCD camera (Princeton Instruments) and analyzed using Metamorph image analysis software. Statistical analyses of neurofilament transport rates were performed using One-way ANOVA tests. The rate of transport was calculated using linear regression analysis.

L-Glutamate was obtained from Sigma Chemical Co. Nifedipine (Calbiochem) was prepared as a 1-mM stock solution in DMSO; MK-801 and CNQX (6-cyano-7-nitroquinoxaline-2,3-dione disodium; both from RBI) were prepared as 1- and 5-mM stock solutions, respectively, in water. Mitochondrial membrane potential was assessed by staining cells with MitoTracker red (Molecular Probes) as previously described (Krohn et al., 1999).

SDS-PAGE and Immunoblot Analyses

Primary cortical neurons were processed for SDS-PAGE by washing twice with ice-cold PBS and scraping into ice-cold 50 mM Tris-HCl, pH 6.8, containing 5 mM EDTA, 5 mM EGTA, 6.25 μg/ml leupeptin, 5 μg/ml aprotinin, 1.2 μg/ml pepstatin A, 1 mM PMSF, 50 μM sodium orthovanadate, and 50 μM sodium fluoride. SDS-PAGE sample buffer was added, and the samples were immediately heated in a boiling water bath. Samples were separated on 12% (wt/vol) acrylamide gels and transferred to Protran nitrocellulose membranes (Schleicher & Schuell) using a Bio-Rad TransBlot system. The blots were probed with antibody M12320 (Transduction Laboratories) that detects total (active and inactive) p42/p44MAPK; anti-active p42/p44MAPK antibody (Promega); antibodies NA1216 and NA1211 (Affiniti) that detect both phosphorylated and nonphosphorylated NF-M and NF-H respectively; NF-L antibody NR4 and antibody DM1A (Sigma Chemical Co.) to tubulin. After washes, the blots were incubated with HRP-conjugated anti-mouse or anti-rabbit Igs (Amersham Pharmacia Biotech), and the blots were developed using an enhanced chemiluminescence system (Amersham Pharmacia Biotech) according to the manufacturer's instructions.

In Vitro Phosphorylation of NF-M Side-arms by Mitogen-activated Protein Kinase and Stress-activated Protein Kinase

Sequences encoding the side-arm domain of rat NF-M were generated by PCR using *Pfu* polymerase and primers 5′-CGCAGGATCCACATTTTCAGGAAGCATCACTGGG-3′ and 5′-CGCAGGATCCTTAGTCACCCTGGGTGACTTCCTT-3′. These primers contain BamHI sites that facilitated the cloning of the domain into the glutathione-S-transferase (GST) fusion vector pGEX-4T-3 (Amersham Pharmacia Biotech). The multiphosphorylation repeat (MPR) domain of the NF-H side-arm cloned into pGEX-3X was as described (Brownlees et al., 2000). GST, GST-NF-M side-arm, and the GST-NF-H MPR domain were expressed in *Escherichia coli* BL21 as described previously (Brownlees et al., 2000). Proteins were assayed using a Bio-Rad protein assay kit according to the manufacturer's instructions.

NF-M side-arm and NF-H MPR domains were phosphorylated by recombinant MAPK or stress-activated protein kinase (SAPK/JNK3; Stratagene) essentially according to the manufacturer's instructions. In brief, equimolar amounts (34 pmol) of each substrate were incubated for 60 min at 30°C with 0.185 MBq γ-[^{32}P]ATP in 25 mM Hepes, pH 7.5, containing 10 mM magnesium acetate, 50 μM ATP, and either 0.02 μg MAPK or 0.125 μg SAPK in a final volume of 20 μl. Reactions were stopped by the addition of SDS sample buffer, and the samples were analyzed by SDS-PAGE and autoradiography.

Results

Transfected EGFP-NF-M Assembles into Normal Neurofilaments in SW13− Cells and Neurons

We chose to study axonal transport of NF-M since NF-L and NF-M are coordinately expressed before NF-H in ro-

dent neurons (Julien et al., 1986; Carden et al., 1987). Therefore, NF-M is probably a constituent of most cellular neurofilaments. Additionally, exogenous-tagged NF-M has been successfully used to measure neurofilament transport in previous studies (Terada et al., 1996; Wang et al., 2000). We tagged rat NF-M at its NH_2 terminus with EGFP. To demonstrate that this NH_2-terminal addition of EGFP does not influence NF-M assembly properties, we studied EGFP-NF-M assembly in transfected SW13− cells that do not express intermediate filaments and in transfected primary cortical neurons.

Transfection of EGFP-NF-M alone into SW13− cells resulted in the formation of NF-M–containing aggregates but not NF-M intermediate filament networks (data not shown). This is consistent with previous observations on rodent neurofilament assembly properties that demonstrate that the formation of NF-M–containing neurofilaments requires coexpression with NF-L (Ching and Liem, 1993; Lee et al., 1993). However, cotransfection of EGFP-NF-M with NF-L led to filament formation (Fig. 1, a and b) that was not noticeably different from filaments formed by cotransfection of NF-L and untagged-NF-M (Fig. 1, c and d). Additionally, experiments involving cotransfection of EGFP-NF-M with NF-L and NF-H, with NF-L and NF-M, and with NF-L, NF-M, and NF-H, all produced intermediate filament networks of normal appearance (all data not shown but see Fig. 1, e and f, for networks in cells cotransfected with EGFP-NF-M and all three untagged neurofilament subunits).

To determine whether EGFP-NF-M was also capable of incorporation into neurofilaments in neurons, we analyzed neurofilament networks in EGFP-NF-M–transfected rat cortical neurons. Here, EGFP-NF-M colocalized with NF-L in typical neurofilament networks (Fig. 1, g and h). Thus, NH_2-terminal tagging of NF-M with EGFP has no noticeable effect on its ability to coassemble into neurofilaments in both SW13− cells and neurons. These observations are consistent with similar assembly studies of vimentin and NF-M, which also involved NH_2-terminal GFP-tagging of these proteins (Ho et al., 1998; Yoon et al., 1998; Wang et al., 2000).

Transfected EGFP-NF-M Is Transported through Neurites at Rates Consistent with that of Slow Axonal Transport in Cultured Neurons, and Transport Requires Metabolic Energy

To study anterograde transport of EGFP-NF-M through neurites, we transfected rat cortical neurons with the EGFP-NF-M plasmid, and 140 min after transfection, analyzed cells by fluorescence microscopy after fixation at 20-min intervals for periods of up to 280 min following transfection. Images of transfected cells were captured, and the distance traveled by EGFP-NF-M at each time point was measured. In these studies, measurements of the distance traveled by EGFP-NF-M were taken from the cell body to the front of the fluorescent signal and were of the longest distances in each neuron. The fluorescent front was taken as the most distal point at which fluorescence above background was detected. For neurites that exhibited branching, measurements were of the major neurite as determined by the length and brightness of fluorescence. To verify the objectivity of the measurements, two independent observers determined the distance to the fluorescent front in the same selected transfected neurons, and the results were not significantly different. Cells were routinely counterstained with Hoechst 33258 to assess nuclear morphology and apoptosis. These studies revealed no nuclear abnormalities or increased cell death associated with the transfected cells, which is in agreement with previous studies of cortical neurons using this transfection method (Nikolic et al., 1996).

Images of at least 20 transfected neurons for each time point were used to calculate the average rate of transport

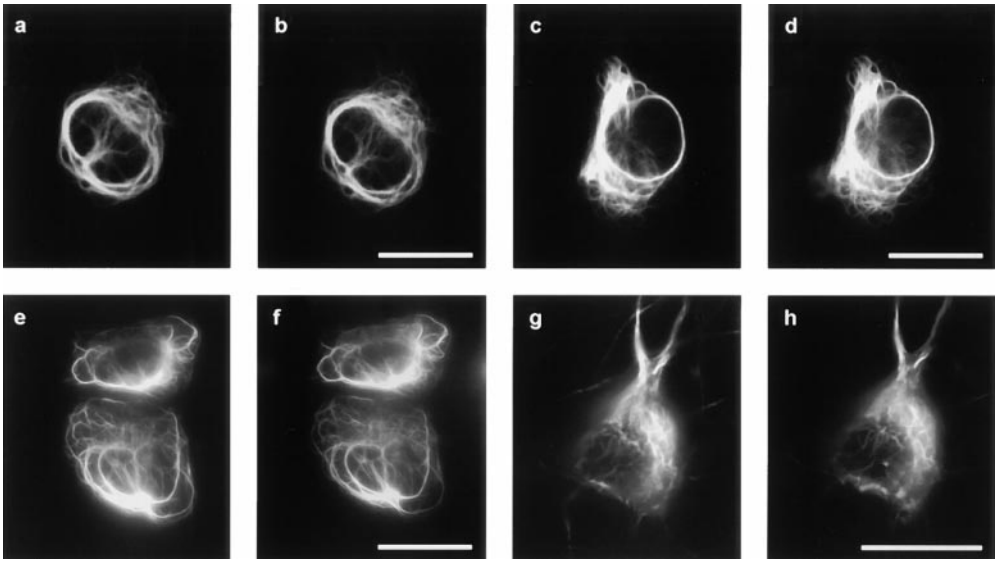

Figure 1. EGFP-NF-M assembly in transfected SW13− cells and 7-d-old primary rat cortical neurons. (a and b) SW13− cells cotransfected with EGFP-NF-M and NF-L; a shows NF-L and b shows EGFP-NF-M. (c and d) SW13− cells cotransfected with NF-L and NF-M; c shows NF-L and d shows NF-M. (e and f) SW13− cells transfected with NF-L, NF-M, NF-H, and EGFP-NF-M; e shows NF-L and f shows EGFP-NF-M. (g and h) Rat cortical neurons transfected with EGFP-NF-M; g shows NF-L and h shows EGFP-NF-M. Although only NF-L and EGFP-NF-M staining are shown in e and f, staining of similarly transfected cells with antibodies to either NF-L and NF-M, NF-L or NF-H, and EGFP-NF-M and NF-H revealed that >90% of cells express both plasmids. Thus, most cells appear to take up and express all three neurofilament subunits in these experiments. Bars, 25 μm.

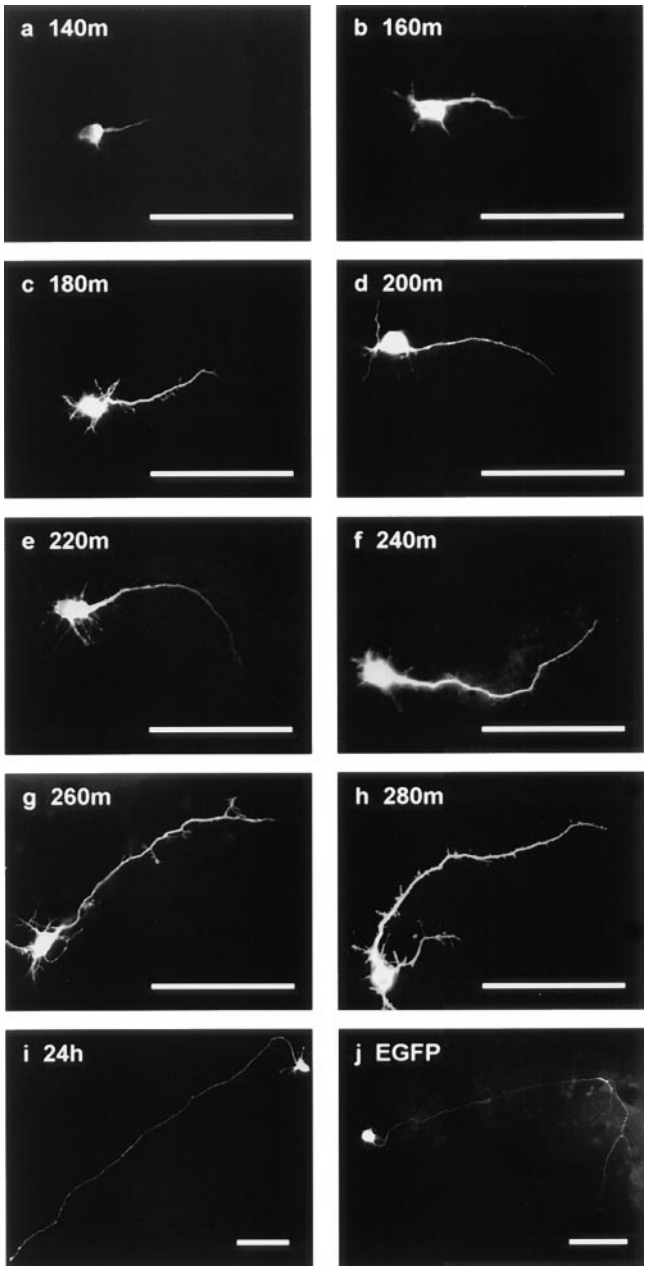

Figure 2. Transport of EGFP-NF-M in transfected cortical neurons. Representative images of EGFP-NF-M–transfected cortical neurons at (a) 140, (b) 160, (c) 180, (d) 200, (e) 220, (f) 240, (g) 260, and (h) 280 min, and (i) 24 h after transfection are shown. (j) Also shown is an EGFP-transfected neuron 240 min after transfection. Bars, 100 μm.

of EGFP-NF-M in each experiment (Fig. 2, representative images of transfected cells at 140–280 min after transfection and also 24 h after transfection). Since we measured the distance traveled by EGFP-NF-M for only up to 300 μm from the cell body, and since the average length of the major neurites in the transfected cortical neurons exceeded 700 μm, the assays are of transport within neurites and are not a reflection of EGFP-NF-M in neurite terminals and neurite growth rates. The average length of neurites in the cultures and also their rate of growth was determined by transfection of β-galactosidase and staining for this enzyme 24 h later. β-Galactosidase has been used on many occasions to determine the shape of neurons, and is known to be present in growth cones (Nikolic et al., 1996). These studies demonstrated that the average length of neurites 24 and 28 h after transfection was 777.5 ± 25.1 μm and 780.3 ± 21.8 μm, respectively (not significantly different using One-way ANOVA test; $P = 0.932$).

From these analyses, we calculated that the average rate of transport of EGFP-NF-M was 80 ± 2 μm/h (Fig. 3). Although this rate of transport of EGFP-NF-M showed no noticeable differences between experiments (compare, for example, the rate of transport of EGFP-NF-M in Figs. 3 and 4, which are from two different experiments), the average distance traveled at the first time point (140 min) differed by ~15 μm between experiments. We attribute this to differences between transfections for each experiment that result in small variations in the precise time at which EGFP-NF-M is first expressed. Indeed, the period of incubation with the DNA/calcium phosphate precipitate during transfection varies by ~10 min depending on the time in which a particular precipitate takes to form on the cells (see Materials and Methods). This 10-min variation is in keeping with the differences observed between experiments in the average distance traveled by EGFP-NF-M at each time point. Other groups have also reported that the time taken for DNA/calcium phosphate precipitates to form on neurons using this transfection method is variable and can lead to small differences in the incubation period (Xia et al., 1996). However, to facilitate comparisons between different experiments, we have adjusted the displayed figures (Figs. 3 and 4) so that the distance traveled by EGFP-NF-M is calculated as the distance from the first measurement (i.e., 140 min after transfection); the distance traveled at this first data point is, therefore, recorded as zero.

To determine whether transport of EGFP-NF-M requires metabolic energy, measurements were taken from cells treated for 30 min with 50 mM 2-deoxy-D-glucose/

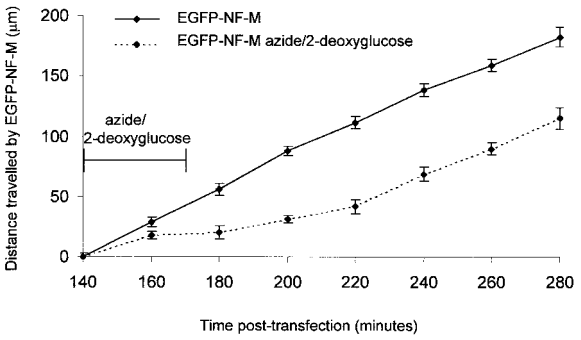

Figure 3. Analyses of EGFP-NF-M transport in transfected neurons. Points shown are distances traveled by EGFP-NF-M at 140–280 min after transfection. For 2-deoxy-D-glucose/sodium azide treatment, cells were treated for the first 30 min. The data sets shown are from one representative experiment and error bars are SEM. One-way ANOVA tests showed significant differences between untreated and 2-deoxy-D-glucose/sodium azide–treated neurons at the 160-min time point ($P = 0.026$) and at all later time points ($P < 0.001$).

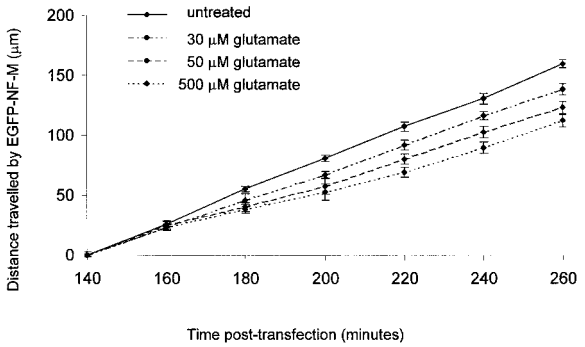

Figure 4. Glutamate inhibits EGFP-NF-M transport in transfected neurons. Points shown are distances traveled by EGFP-NF-M at 140–260 min after transfection. Cells were untreated or treated with 500, 50, or 30 μM glutamate. Glutamate was applied at the 140-min time point. The data sets shown are from one representative experiment and error bars are SEM. One-way ANOVA tests revealed no significant differences between untreated and glutamate-treated neurons at the 160-min time point (untreated versus 30 μM glutamate, $P = 0.285$; untreated versus 50 μM glutamate, $P = 0.701$; untreated versus 500 μM glutamate, $P = 0.447$). Significant differences between untreated and both 500 μM glutamate ($P < 0.001$) and 50 μM glutamate ($P < 0.001$), but not 30 μM glutamate ($P = 0.132$), treatments were detected at the 180-min time point. At later time points, significant differences were detected between untreated and all glutamate treatments ($P < 0.001$).

0.05% sodium azide, 140 min after transfection. This treatment is known to halt energy-dependent processes including motile properties of transfected vimentin in living cells (Yoon et al., 1998); 2-deoxy-D-glucose inhibits glycolysis at an early step, whereas sodium azide inhibits electron transport at the last step. 2-Deoxy-D-glucose/sodium azide retarded transport but, after washout and a recovery period, EGFP-NF-M movement resumed at a rate that was not noticeably different from that of untreated cells (Fig. 3). The absence of a complete arrest to EGFP-NF-M movement at the 160-min time point may be because uptake of 2-deoxy-D-glucose/0.05% sodium azide and inhibition of metabolic processes takes some minutes. These observations are similar to those seen in GFP-vimentin–transfected fibroblasts, where 2-deoxy-D-glucose/sodium azide also halts motility but, after washout and a similar recovery period, vimentin movements resume (Yoon et al., 1998).

For comparison, we also studied anterograde movement of transfected EGFP in cortical neurons since there is no evidence to suggest that EGFP is transported by slow axonal transport and it might, therefore, move at a different rate. In contrast to EGFP-NF-M, EGFP was detected along the length of neurites at the time point assayed (240 min after transfection; Fig. 2 j). This indicates that a proportion of EGFP may move by fast transport mechanisms since this rate of movement is probably incompatible with simple diffusion (Sabry et al., 1995). This observation also suggests that, in the EGFP-NF-M transfections, EGFP remains covalently attached to NF-M and has not been released by a proteolytic event. Thus, transfected EGFP-NF-M is transported through neurites of cultured primary cortical neurons at ~80 μm/h, a rate different to that of EGFP and consistent with the known rates of slow axonal transport, and this movement requires metabolic energy.

Glutamate Inhibits Transport of Transfected EGFP-NF-M

To study how the treatment of neurons with glutamate influenced EGFP-NF-M transport rates, we treated cells with 500, 50, and 30 μM glutamate. Glutamate treatment was applied 140 min after transfection (i.e., at the same time as the first recording of distance traveled was made) and maintained over the course of the experiment. 7-d-old cortical neurons are known to be susceptible to glutamate treatment and to express glutamate receptors (Cheng et al., 1994; Davis et al., 1995). Although glutamate had no significant effect on EGFP-NF-M movement over the first 20 min, at later time points, a significant inhibition of transport was observed. The extent of this inhibition of EGFP-NF-M transport was related to the concentration of glutamate applied to the cultures (Fig. 4).

Previous studies have shown that treatment of cultured cortical neurons with concentrations of up to 1 mM glutamate, for periods in excess of the times used here, does not influence cell viability (Davis et al., 1995). Indeed, the Hoechst 33258 staining that we routinely performed to monitor viability of the cells revealed no evidence of increased cell death over the period of treatment. However, to confirm that the slowing of EGFP-NF-M transport was not due to a simple loss of viability of the cells, we performed lactate dehydrogenase cell viability assays on glutamate-treated cells for periods of up to 180 min (i.e., longer than the 120-min period in which EGFP-NF-M transport was studied in the presence of glutamate). These studies revealed that there was no significant loss of viability over the time course of the experiment (data not shown), which is in agreement with previous reports of glutamate-treated cortical neurons (Davis et al., 1995).

To further confirm that this slowing of EGFP-NF-M transport was induced by the glutamate treatment, and to determine which glutamate receptor subtype(s) might mediate this effect, we studied EGFP-NF-M transport in either untreated or 50 μM glutamate-treated neurons, in the presence or absence of ionic glutamate receptor antagonists. Treatment with 5 μM CNQX (AMPA/kainate receptor blocker) had no significant effect on glutamate-induced retardation of the distance traveled; however, 1 μM MK-801 (NMDA receptor blocker) completely inhibited the effect of glutamate (Fig. 5). We also treated cells with 1 μM nifedipine, an inhibitor of L-type voltage-gated calcium channels, which are activated after depolarization of the postsynaptic membrane (Ghosh and Greenberg, 1995). However, nifedipine had no effect on glutamate-induced slowing of EGFP-NF-M transport (Fig. 5).

We also studied whether glutamate induced changes in the levels of NF-L, NF-M, and NF-H or tubulin proteins in the neurons by immunoblotting (Fig. 6). However, no alterations to the steady state levels of any of these proteins were detected. Finally, we assessed the mitochondrial membrane potential after glutamate treatment by staining with the probe MitoTracker red. These studies did not reveal any changes to mitochondria in response to gluta-

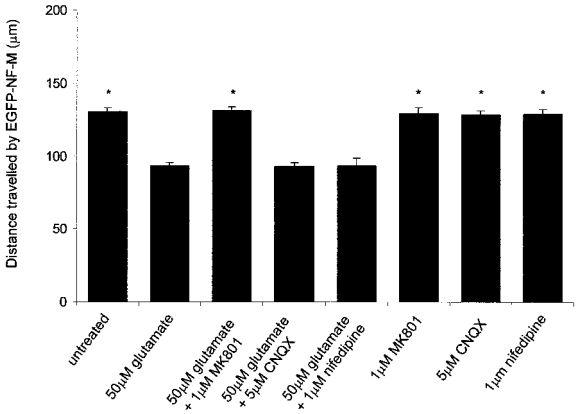

Figure 5. Effect of glutamate receptor antagonists on glutamate-induced inhibition of EGFP-NF-M transport. Histogram shows distance traveled by EGFP-NF-M 240 min after transfection in either untreated or 50-μM glutamate-treated neurons in the presence or absence of 1 μM MK-801, 5 μM CNQX, or 1 μM nifedipine. Glutamate was applied at the 140-min time point and inhibitors 10 min before this. Data from one representative experiment are shown. Asterisks indicate treatments that display significant differences ($P < 0.001$) compared with 50-μM glutamate treatment as analyzed by One-way ANOVA tests. No significant difference was observed between untreated neurons and neurons treated with glutamate in the presence of MK801. Error bars are SEM.

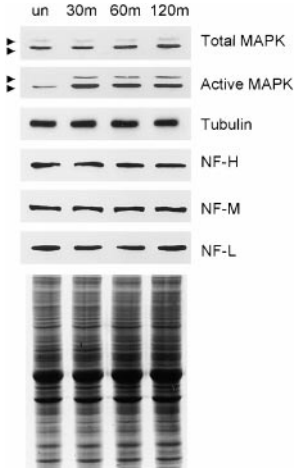

Figure 6. Glutamate activates p42 and p44 MAPKs and does not alter the levels of neurofilament or tubulin proteins in cortical neurons. 7-d-old cortical neurons were either untreated (un), or treated with 100 μM glutamate for 30, 60, or 120 min, and then analyzed by 12% SDS-PAGE and immunoblotting. No change in the total levels of either p42 or p44 MAPK (arrowheads), but a noticeable increase in the active forms of both these kinases was observed after glutamate treatment. Glutamate did not alter the levels of NF-L, NF-M, NF-H, or tubulin. An identically loaded Coomassie-stained gel is shown at the bottom to demonstrate equal protein loading of the samples.

mate over the time periods used for investigating EGFP-NF-M transport (data not shown). Thus, over the time course studied, glutamate retards anterograde transport of EGFP-NF-M in cultured cortical neurons without affecting cell viability or neurofilament protein levels, and this effect is mediated at least, in part, through NMDA-type glutamate receptors.

Glutamate Activates Members of the MAP Kinase Family and Induces Increased Phosphorylation of NF-M/NF-H Side-arms, and NF-M/NF-H Side-arms Are Substrates for MAP Kinases

Many studies have shown that increased phosphorylation of NF-M and NF-H side-arms is associated with a slowing of neurofilament transport (Watson et al., 1989a,b, 1991; Archer et al., 1994; Nixon et al., 1994a,b; Jung and Shea, 1999). Since glutamate is known to activate a number of kinases in neurons (see below), the slowing in the rate of EGFP-NF-M transport observed in response to glutamate may be due (at least in part) to increased phosphorylation of neurofilament side-arms. Much of the phosphate that is incorporated into NF-M/NF-H side-arms is on serines within the motif Lys-Ser-Pro, and this suggests that the responsible kinases are proline-directed kinases. Proline-directed kinases that have been shown to phosphorylate NF-M/NF-H side-arms include cyclin-dependent kinase-5 (cdk5), glycogen synthase kinase-3, and members of the MAPK family including p42/p44MAPK and SAPK1b/c (Guan et al., 1991; Lew et al., 1992; Hisanaga et al., 1993; Miyasaka et al., 1993; Shetty et al., 1993; Giasson and Mushynski, 1996, 1997; Guidato et al., 1996; Sun et al., 1996; Bajaj and Miller, 1997; Li et al., 1999; Veeranna et al., 1998; Brownlees et al., 2000).

We have recently demonstrated that, in rat cortical neurons (as used here), glutamate activates SAPK1b but has no effect on cdk5 activity and causes a decrease in glycogen synthase kinase-3 activity (Brownlees et al., 2000). Others have also shown that glutamate activates SAPKs in neurons (Bading and Greenberg, 1991; Kurino et al., 1995; Xia et al., 1996; Kawasaki et al., 1997; Schwarzschild et al., 1997, 1999). However, we did not investigate the effect that glutamate has on p42/p44MAPK activities in our earlier studies, and rectified this omission by the use of antibodies that detect total and active p42/p44MAPK. These studies demonstrated that glutamate induced a marked activation of both MAPK isoforms, and that this activation extended for at least 120 min (i.e., the time course over which EGFP-NF-M transport was studied; Fig. 6). Others have also shown that glutamate can activate p42/p44-MAPK in neurons (Bading and Greenberg, 1991; Kurino et al., 1995; Xia et al., 1996; Schwarzschild et al., 1999). Thus, p42/p44MAPK and SAPKs are good candidates for altering NF-M/NF-H side-arm domain phosphorylation in response to glutamate.

We also studied the subcellular localization of active p42/p44MAPK and SAPKs in the neurons using antibodies that detect the active forms of these kinases. In untreated cells, active p42/p44MAPK was only weakly detected where it localized to cell bodies and some neurites (Fig. 7 a); active SAPK was present mainly in neurites (Fig. 7 c). Treatment with glutamate induced a marked increase in active p42/p44MAPK labeling in both cell bodies (including some nuclei) and neurites (Fig. 7 b). Similarly, glutamate also increased labeling for active SAPKs, particularly in cell bodies and nuclei (Fig. 7 d).

NF-M side-arms are phosphorylated by p42/p44MAPK (Veeranna et al., 1998; Li et al., 1999) and SAPK1b, which is a major SAPK in neurons (Mohit et al., 1995; Martin et al., 1996; Carboni et al., 1997, 1998; Lee et al., 1999), has been shown to phosphorylate NF-H side-arms (Brownlees et al., 2000). However, there is currently little data to demonstrate that SAPK1b will phosphorylate NF-M side-arms. Therefore, we prepared the side-arm domain of NF-M as a GST fusion protein and tested its ability to be phosphory-

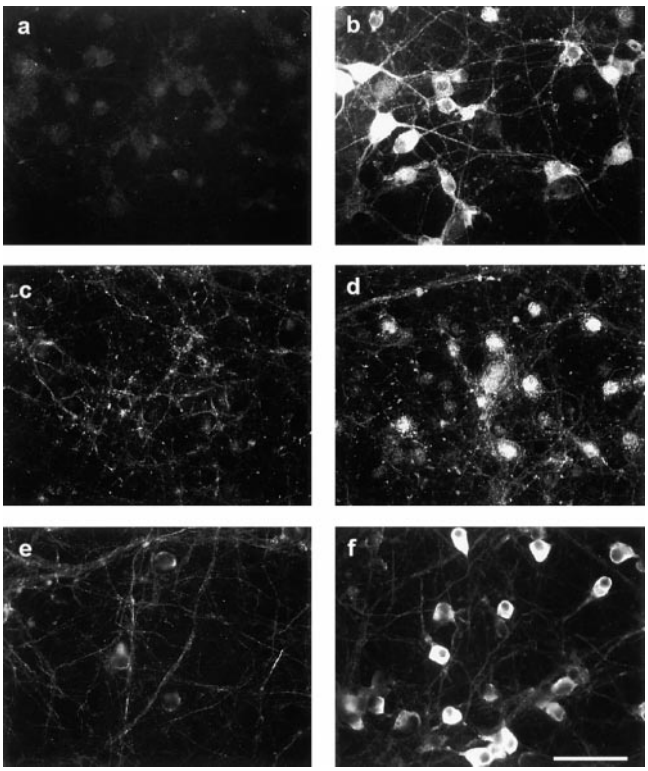

Figure 7. Localization of active p42/p44MAPK, SAPKs, and phosphorylated NF-M/NF-H side-arms (SMI36 labeling) in untreated and glutamate-treated 7-d-old cortical neurons. a, c, and e are untreated cells; b, d, and f are treated with 100 μM glutamate for 30 min. Increased labeling for active p42/p44MAPK (a and b) and SAPKs (c and d) is seen after glutamate treatment. SMI36 labeling is markedly increased in cell bodies after glutamate exposure (e and f). Bar, 25 μm.

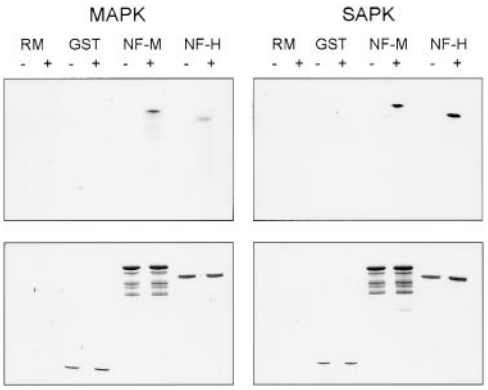

Figure 8. In vitro phosphorylation of NF-M side-arm and the MPR domain of NF-H side-arm with p42MAPK and SAPK1b. Left panels are phosphorylation by p42MAPK, and right panels are phosphorylation using SAPK1b. The top panels are the autoradiographs, and the bottom panels are the corresponding Coomassie-stained gels. RM are reaction mixes only without GST/NF-M/NF-H substrates; GST are reaction mixes with GST substrate; NF-M are reaction mixes with NF-M substrate; and NF-H are reaction mixes with the NF-H MPR domain substrate. Minus and plus signs refer to the absence or inclusion of kinases in the reaction mixes. The lower molecular mass species seen in tracks containing the NF-M side-arm domain are probably proteolytic degradation products since many of these react with NF-M antibodies. We were unable to inhibit this proteolysis despite using cocktails of protease inhibitors.

lated by recombinant SAPK1b. For comparisons, we also used as a substrate the MPR domain of NF-H side-arms that contains the Lys-Ser-Pro repeat region (Brownlees et al., 2000) and recombinant p42MAPK. Both NF-M and NF-H substrates, but not GST, were phosphorylated by p42MAPK and SAPK1b (Fig. 8). Not all Ser-Thr-Pro motifs are phosphorylated under these conditions, since we have shown that Thr668 in the Alzheimer's disease amyloid precursor protein, which is a known in vivo phosphorylation site, is not phosphorylated by MAPK (Aplin et al., 1996).

We next examined if glutamate induced alterations to the phosphorylation of NF-M/H side-arms in vivo in cortical neurons. SMI36, an antibody that reacts with phosphorylated but not nonphosphorylated NF-M/NF-H side-arms (Sternberger and Sternberger, 1983), labeled neurites but only weakly labeled cell bodies in untreated cells (Fig. 7 e). This is consistent with many studies, which have shown that NF-M and NF-H side-arms are heavily phosphorylated in axons but are much less phosphorylated in cell bodies and proximal axons (Julien and Mushynski, 1982; Sternberger and Sternberger, 1983; Carden et al., 1985; Lee et al., 1987, 1988; Nixon et al., 1994b). However, glutamate induced a marked increase in SMI36 labeling of cell bodies that was evident as early as 30 min after glutamate treatment (Fig. 7 f). We also confirmed that glutamate induced an increased cell body phosphorylation of NF-M/NF-H side-arms in the EGFP-NF-M–transfected neurons by the staining of transfected cultures with SMI36 (Fig. 9, a–d). Thus, glutamate activates members of the MAP kinase family including p42/p44MAPK and SAPK1b, neurofilament side-arm domains are substrates for these kinases, and glutamate induces increased phosphorylation of neurofilament side-arms in cell bodies of cortical neurons.

Finally, we analyzed whether the glutamate-induced slowing of EGFP-NF-M transport might lead to the formation of neurofilament accumulations such as are seen in some neurodegenerative diseases. Accumulations typical of these disorders were rarely detected over the time course in which transport rates were studied (140–260 min after transfection and 120-min glutamate treatment). However, after 180 min of glutamate treatment (i.e., 320 min after transfection), increased EGFP-NF-M labeling and swelling of proximal neurites become more noticeable in a proportion of the neurons. To quantify this more carefully, we randomly captured images of EGFP-NF-M–transfected cells either untreated or treated with 100 μM glutamate at this time point and scored them blind for the presence of accumulations. In two different experiments, accumulations typical of the ones shown in Fig. 10 (see also accumulation in Fig. 9 double labeled with SMI36) were found in greater numbers in the glutamate-treated cells (experiment 1, 29.6% treated [$n = 81$] versus 7.6% untreated [$n = 92$]; experiment 2, 33.3% treated [$n = 69$] versus 9.9% [$n = 111$]). The accumulations seen in untreated neurons may be a consequence of increased ex-

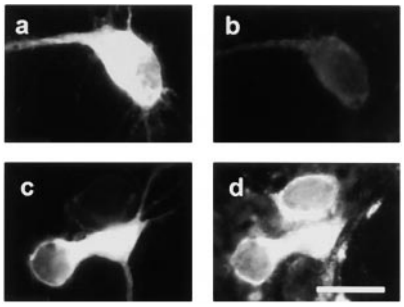

Figure 9. Glutamate induces increased phosphorylation of NF-M/NF-H side-arms in cell bodies of EGFP-NF-M–transfected neurons. Cells were transfected with EGFP-NF-M and, 320 min after transfection, were fixed and immunostained with SMI36. a and b are untreated; c and d are treated with 100 μM glutamate for 180 min. a and c show EGFP-NF-M; b and d show SMI36 labeling. Note the proximal accumulation of neurofilament protein in the glutamate-treated cell. Bar, 25 μm.

pression of EGFP-NF-M since overexpression of NF-M in transgenic mice can also lead to neurofilament accumulations (Vickers et al., 1994; Wong et al., 1995).

Discussion

Anterograde axonal transport of the cytoskeleton has been studied using a variety of experimental systems both in vivo and in cultured cells (for reviews see Baas and Brown, 1997; Hirokawa et al., 1997; Nixon, 1998). These include monitoring the movement of radiolabeled proteins (Reinsch et al., 1991; de Waegh et al., 1992; Lasek et al., 1992; Archer et al., 1994; Nixon et al., 1994b; Collard et al., 1995; Campenot et al., 1996; Zhang et al., 1997; Williamson and Cleveland, 1999), the use of fluorescently labeled cytoskeletal proteins, and photoactivation and photobleaching techniques (Keith, 1987; Okabe and Hirokawa, 1992, 1993; Okabe et al., 1993; Takeda et al., 1994, 1995; Sabry et al., 1995; Funakoshi et al., 1996; Miller and Joshi, 1996; Yu et al., 1996), analyses of cytoskeletal accumulation after physical constriction of axons (Koehnle and Brown, 1999), and, finally, studies of labeled cytoskeletal proteins introduced into neurons using recombinant DNA methodologies (Terada et al., 1996; Yabe et al., 1999; Wang et al., 2000). The new method that we describe here complements these existing techniques and offers certain advantages. First, it can be applied to any cytoskeletal protein whose properties are not influenced by tagging with EGFP. Second, since it involves transfection of cytoskeletal cDNAs, analyses of mutants and the effect of overexpression of other proteins that might influence transport by cotransfection methods are possible. Third, the effects that various physiological agents have on slow axonal transport are easily studied (such as we have described here with glutamate and glutamate receptor antagonists). Finally, the method is not technically demanding and is simple to perform; the fluorescent front is discrete and easily observed and the error bars for distance traveled by EGFP-NF-M are small and this testifies to the quality of the data. Thus, our method is simple and robust.

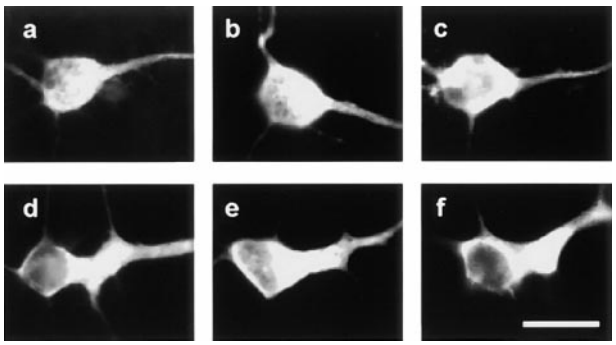

Figure 10. EGFP-NF-M accumulations begin to develop in proximal neurites of some transfected neurons treated with 100 μM glutamate for 180 min (i.e., 320 min after transfection). Images shown are of EGFP-NF-M in proximal regions of neurites 320 min after transfection in untreated cells (a–c) and cells treated with 100 μM glutamate for 180 min and in which neurofilament accumulations are starting to develop (d–f). Bar, 25 μm.

In vivo, neurofilament transport rates vary between ~10–125 μm/h depending on the type of neuron, age of the animal, and location within the axon (Lee and Cleveland, 1996; Baas and Brown, 1997; Hirokawa et al., 1997; Nixon, 1998). However, recent cellular studies have shown that neurofilaments travel at fast transport rates (up to 2.3 μm/s), but that this movement is interrupted by prolonged pauses (Wang et al., 2000). Therefore, only a proportion of neurofilaments are moving at any one time (estimated as 1–15%), such that an overall slow transport rate is observed. Since we analyzed EGFP-NF-M movement in cells fixed at 20-min intervals rather than in living cells, our assays calculate this overall slow transport rate. In the cortical cells used, this is 80 ± 2 μm/h, which is consistent with the known rates of transport as assayed in vivo by other methods.

Abnormal accumulations of neurofilament proteins are seen in ALS, Alzheimer's disease, and Lewy bodies in Parkinson's disease and Lewy body dementia (Hirano, 1991; Trojanowski et al., 1993; Schmidt et al., 1996). Such accumulations suggest that the transport of neurofilament proteins through axons is disrupted in these disease states. Indeed, measurements of axonal transport in several transgenic mouse models of ALS reveal that the slowing of cytoskeletal transport is an early pathological feature (Collard et al., 1995; Zhang et al., 1997; Williamson and Cleveland, 1999).

The events that lead to cell death in these neurodegenerative diseases are not known, but excitotoxic mechanisms involving glutamate have been suggested to be part of the disease process for both ALS (for reviews see Shaw, 1994; Rothstein, 1996) and Alzheimer's disease (Guo et al., 1999). Indeed, a loss of the glial glutamate transporter (EAAT2) has been described in sporadic forms of ALS (Lin et al., 1998) and in a transgenic mouse model of ALS (Bruijn et al., 1997). Moreover, mutant SOD1s, which cause familial forms of ALS, induce selective damage to EAAT2 by oxidative mechanisms (Trotti et al., 1999); uptake of glutamate via sodium-dependent glutamate transporters is a primary mechanism for inactivation of extracellular glutamate. Thus, glutamate-induced excitotoxicity might be part of the pathogenic process in several neuro-

degenerative diseases. Our finding that glutamate inhibits anterograde axonal transport of NF-M, therefore, provides a mechanism to link excitotoxicity with neurofilament accumulation in these disorders.

The series of molecular events by which glutamate exposure might lead to a slowing of neurofilament transport are not clear. However, increased phosphorylation of NF-M and NF-H side-arm domains has been associated with slower neurofilament transport rates in many studies (Watson et al., 1989a,b, 1991; Archer et al., 1994; Nixon et al., 1994a,b; Jung and Shea, 1999). Therefore, it is notable that we observe an increase in neurofilament side-arm phosphorylation in cell bodies after glutamate treatment. Other studies have shown that glutamate can cause increased neurofilament side-arm phosphorylation in neurons (Asahara et al., 1999; Brownlees et al., 2000). NF-M and NF-H side-arms are more heavily phosphorylated in axons than cell bodies (Julien and Mushynski, 1982; Sternberger and Sternberger, 1983; Carden et al., 1985; Lee et al., 1987, 1988; Nixon et al., 1994b), and so it is also possible that changes to neurofilament phosphorylation occurred in neurites but were not so easily detectable. Glutamate is known to activate members of the MAPK family including p42/p44MAPK and SAPKs (Bading and Greenberg, 1991; Kurino et al., 1995; Xia et al., 1996; Schwarzschild et al., 1997, 1999; Brownlees et al., 2000), and we demonstrate that this is also the case in the cortical neurons used here. p42/p44MAPK and SAPK1b/c will all phosphorylate NF-M/NF-H side-arms (Giasson and Mushynski, 1996, 1997; Veeranna et al., 1998; Li et al., 1999; Brownlees et al., 2000; data shown here), and we show that the active forms of these kinases are present in cell bodies in the glutamate-treated neurons. Together, these observations suggest that these particular kinases are the link between glutamate and increased neurofilament phosphorylation.

Thus, activation of p42/p44MAPK and SAPKs, and phosphorylation of NF-M/NF-H side-arms might be at least part of the process by which glutamate causes a slowing of neurofilament transport in the cortical neurons used here. Whether the same processes occur in other neuronal cell types including lower motor neurons remains to be established. However, other possible mechanisms including glutamate-induced alterations to the neurofilament transport motor, which has to date not been identified, or the way in which neurofilaments attach to the motor, which is again not known (Brady, 2000), cannot be excluded. Indeed, one recent suggestion is that NF-M/NF-H side-arm phosphorylation regulates association of neurofilaments with kinesin, a fast motor (Yabe et al., 2000). Whatever the precise mechanism, the results presented here are the first to show a link between glutamate excitotoxicity, a proposed pathogenic process for several human neurodegenerative diseases, and slowing of neurofilament transport, which is a pathological feature in at least some of these disorders.

We thank Ron Leim (Columbia University, New York) for rat NF-L, NF-M, and NF-H cDNAs.

This work was funded by grants from the United Kingdom Motor Neurone Disease Association, The Wellcome Trust, and Kings Healthcare Trust. Steven Ackerley holds The Jim Tew Memorial Studentship, funded by the UK Motor Neurone Disease Association.

Submitted: 7 December 1999
Revised: 5 June 2000
Accepted: 5 June 2000

References

Aplin, A.E., G.M. Gibb, J.S. Jacobsen, J.-M. Gallo, and B.H. Anderton. 1996. In vitro phosphorylation of the cytoplasmic domain of the amyloid precursor protein by glycogen synthase kinase-3β. *J. Neurochem.* 67:699–707.

Archer, D.R., D.F. Watson, and J.W. Griffin. 1994. Phosphorylation-dependent immunoreactivity of neurofilaments and the rate of slow axonal transport in the central and peripheral axons of the rat dorsal root ganglia. *J. Neurochem.* 62:1119–1125.

Asahara, H., T. Taniwaki, Y. Ohyagi, T. Yamada, and J. Kira. 1999. Glutamate enhances phosphorylation of neurofilaments in cerebellar granule cell culture. *J. Neurol. Sci.* 171:84–87.

Baas, P.W., and A. Brown. 1997. Slow axonal transport: the polymer transport model. *Trends Cell Biol.* 7:380–384.

Bading, H., and M.E. Greenberg. 1991. Stimulation of protein tyrosine phosphorylation by NMDA receptor activation. *Science.* 253:912–914.

Bajaj, N.P., and C.C.J. Miller. 1997. Phosphorylation of neurofilament heavy-chain side-arm fragments by cyclin-dependent kinase-5 and glycogen synthase kinase-3a in transfected cells. *J. Neurochem.* 69:737–743.

Brady, S.T. 2000. Neurofilaments run in sprints not marathons. *Nat. Cell Biol.* 2:E43–E45.

Brownlees, J., A. Yates, N.P. Bajaj, D. Davis, B.H. Anderton, P.N. Leigh, C.E. Shaw, and C.C.J. Miller. 2000. Phosphorylation of neurofilament heavy chain side-arms by stress activated protein kinase-1b/Jun N-terminal kinase-3. *J. Cell Sci.* 113:401–407.

Bruijn, L.I., M.W. Becher, M.K. Lee, K.L. Anderson, N.A. Jenkins, N.G. Copeland, S.S. Sisodia, J.D. Rothstein, D.R. Borchelt, D.L. Price, and D.W. Cleveland. 1997. ALS-linked SOD1 mutant G85R mediates damage to astrocytes and promotes rapidly progressive disease with SOD1-containing inclusions. *Neuron.* 18:327–338.

Campenot, R.B., K. Lund, and D.L. Senger. 1996. Delivery of newly synthesized tubulin to rapidly growing distal axons of rat sympathetic neurons in compartmentalized cultures. *J. Cell Biol.* 135:701–709.

Carboni, L., S. Tacconi, R. Carletti, E. Bettini, and F. Ferraguti. 1997. Localization of the messenger RNA for the c-Jun NH_2-terminal kinase kinase in the adult and developing rat brain: an in situ hybridization study. *Neuroscience.* 80:147–160.

Carboni, L., R. Carletti, S. Tacconi, C. Corti, and F. Ferraguti. 1998. Differential expression of SAPK isoforms in the rat brain. An in situ hybridisation study in the adult rat brain and during post-natal development. *Mol. Brain Res.* 60:57–68.

Carden, M.J., W.W. Schlaepfer, and V.M. Lee. 1985. The structure, biochemical properties, and immunogenicity of neurofilament peripheral regions are determined by phosphorylation state. *J. Biol. Chem.* 260:9805–9817.

Carden, M.J., J.Q. Trojanowski, W.W. Schlaepfer, and V.M. Lee. 1987. Two-stage expression of neurofilament polypeptides during rat neurogenesis with early establishment of adult phosphorylation patterns. *J. Neurosci.* 7:3489–3504.

Cheng, B., Y. Goodman, J.G. Begley, and M.P. Mattson. 1994. Neurotrophin-4/5 protects hippocampal and cortical neurons against energy deprivation- and excitatory amino acid-induced injury. *Brain Res.* 650:331–335.

Chin, S.S.M., and R.K.H. Liem. 1989. Expression of rat neurofilament proteins NF-L and NF-M in transfected non-neuronal cells. *Eur. J. Cell Biol.* 50:475–490.

Chin, S.S.M., and R.K.H. Liem. 1990. Transfected rat high-molecular-weight neurofilament (NF-H) coassembles with vimentin in a predominantly non-phosphorylated form. *J. Neurosci.* 10:3714–3726.

Ching, G.Y., and R.K. Liem. 1993. Assembly of type IV neuronal intermediate filaments in nonneuronal cells in the absence of preexisting cytoplasmic intermediate filaments. *J. Cell Biol.* 122:1323–1335.

Collard, J.-F., F. Cote, and J.-P. Julien. 1995. Defective axonal transport in a transgenic mouse model of amyotrophic lateral sclerosis. *Nature.* 375:61–64.

Davis, D.R., J.-P. Brion, A.M. Couck, J.-M. Gallo, D.P. Hanger, K. Ladhani, C. Lewis, C.C. Miller, T. Rupniak, C. Smith, and B.H. Anderton. 1995. The phosphorylation state of the microtubule-associated protein tau as affected by glutamate, colchicine and β-amyloid in primary rat cortical neuronal cultures. *Biochem. J.* 309:941–949.

de Waegh, S.M., V.M. Lee, and S.T. Brady. 1992. Local modulation of neurofilament phosphorylation, axonal caliber and slow axonal transport by myelinating Schwann cells. *Cell.* 68:451–463.

Funakoshi, T., S. Takeda, and N. Hirokawa. 1996. Active transport of photoactivated tubulin molecules in growing axons revealed by a new electron microscope analysis. *J. Cell Biol.* 133:1347–1353.

Ghosh, A., and M.E. Greenberg. 1995. Calcium signalling in neurons: molecular mechanisms and cellular consequences. *Science.* 268:239–247.

Giasson, B.I., and W.E. Mushynski. 1996. Aberrant stress-induced phosphorylation of perikaryal neurofilaments. *J. Biol. Chem.* 271:30404–30409.

Giasson, B.I., and W.E. Mushynski. 1997. Study of proline-directed kinases involved in phosphorylation of the heavy neurofilament subunit. *J. Neurosci.*

17:9466–9472.
Gibb, B.J.M., J. Robertson, and C.C.J. Miller. 1996. Assembly properties of neurofilament light chain Ser^{55} mutants in transfected mammalian cells. *J. Neurochem*. 66:1306–1311.
Guan, R.J., B.S. Khatra, and J.A. Cohlberg. 1991. Phosphorylation of bovine neurofilament proteins by protein kinase F_A (glycogen synthase kinase 3). *J. Biol. Chem*. 266:8262–8267.
Guidato, S., L.-H. Tsai, J. Woodgett, and C.C.J. Miller. 1996. Differential cellular phosphorylation of neurofilament heavy side-arms by glycogen synthase kinase-3 and cyclin-dependent kinase-5. *J. Neurochem*. 66:1698–1706.
Guo, Q., W.M. Fu, B.L. Sopher, M.W. Miller, C.B. Ware, G.M. Martin, and M.P. Mattson. 1999. Increased vulnerability of hippocampal neurons to excitotoxic necrosis in presenilin-1 mutant knock-in mice. *Nat. Med*. 5:101–106.
Hirano, A. 1991. Cytopathology of amyotrophic lateral sclerosis. *In* Advances in Neurology. Vol. 56. Amyotrophic lateral sclerosis and other motor neuron diseases. L.P. Rowland, editor. Raven Press, New York. 91–101.
Hirokawa, N., S. Terada, T. Funakoshi, and S. Takeda. 1997. Slow axonal transport: the subunit transport model. *Trends Cell Biol.* 7:384–388.
Hisanaga, S., K. Ishiguro, T. Uchida, E. Okumura, T. Okano, and T. Kishimoto. 1993. Tau protein kinase II has a similar characteristic to cdc2 kinase for phosphorylating neurofilament proteins. *J. Biol. Chem*. 268:15056–15060.
Ho, C.L., J.L. Martys, A. Mikhailov, G.G. Gundersen, and R.K.H. Liem. 1998. Novel features of intermediate filament dynamics revealed by green fluorescent protein chimeras. *J. Cell Sci.* 111:1767–1778.
Julien, J.-P., and W.E. Mushynski. 1982. Multiple phosphorylation sites in mammalian neurofilament polypeptides. *J. Biol. Chem*. 257:10467–10470.
Julien, J.-P., D. Meijer, J. Hurst, and F. Grosveld. 1986. Cloning and developmental expression of the murine neurofilament gene family. *Mol. Brain Res.* 1:243–250.
Jung, C.W., and T.B. Shea. 1999. Regulation of neurofilament axonal transport by phosphorylation in optic axons in situ. *Cell Motil. Cytoskelet.* 42:230–240.
Kawasaki, H., T. Morooka, S. Shimohama, J. Kimura, T. Hirano, Y. Gotoh, and E. Nishida. 1997. Activation and involvement of p38 mitogen-activated protein kinase in glutamate-induced apoptosis in rat cerebellar granule cells. *J. Biol. Chem*. 272:18518–18521.
Keith, C.H. 1987. Slow transport of tubulin in the neurites of differentiated PC12 cells. *Science*. 235:337–339.
Koehnle, T.J., and A. Brown. 1999. Slow axonal transport of neurofilament protein in cultured neurons. *J. Cell Biol.* 144:447–458.
Krohn, A.J., T. Wahlbrink, and J.H.M. Prehn. 1999. Mitochondrial depolarization is not required for neuronal apoptosis. *J. Neurosci.* 19:7394–7404.
Kurino, M., K. Fukunaga, Y. Ushio, and E. Miyamoto. 1995. Activation of mitogen-activated protein kinase in cultured rat hippocampal neurons by stimulation of glutamate receptors. *J. Neurochem*. 65:1282–1289.
Lasek, R.J., P. Paggi, and M.J. Katz. 1992. Slow axonal transport mechanisms move neurofilaments relentlessly in mouse optic axons. *J. Cell Biol.* 117:607–616.
Lee, J.K., J.Y. Park, Y.D. Lee, S.H. Lee, and P.L. Han. 1999. Distinct localization of SAPK isoforms in neurons of adult mouse brain implies multiple signaling modes of SAPK pathway. *Mol. Brain Res.* 70:116–124.
Lee, M.K., and D.W. Cleveland. 1996. Neuronal intermediate filaments. *Annu. Rev. Neurosci.* 19:187–217.
Lee, M.K., Z. Xu, P.C. Wong, and D.W. Cleveland. 1993. Neurofilaments are obligate heteropolymers in vivo. *J. Cell Biol.* 122:1337–1350.
Lee, V.M.-Y., M.J. Carden, W.W. Schlaepfer, and J.Q. Trojanowski. 1987. Monoclonal antibodies distinguish several differently phosphorylated states of the two largest rat neurofilament subunits (NF-H and NF-M) and demonstrate their existence in the normal nervous system of rats. *J. Neurosci.* 7:3474–3488.
Lee, V.M.-Y., L. Otvos, M.J. Carden, M. Hollosi, B. Deitzschold, and R.A. Lazzarini. 1988. Identification of the major multiphosphorylation site in mammalian neurofilaments. *Proc. Natl. Acad. Sci. USA*. 85:1998–2002.
Lew, J., R.J. Winkfein, H.K. Paudel, and J.H. Wang. 1992. Brain proline-directed protein kinase is a neurofilament kinase which displays high sequence homology to $p34^{cdc2}$. *J. Biol. Chem*. 267:25922–25926.
Li, B.S., Veeranna, J.G. Gu, P. Grant, and H.C. Pant. 1999. Activation of mitogen-activated protein kinases (Erk1 and Erk2) cascade results in phosphorylation of NF-M tail domains in transfected NIH 3T3 cells. *Eur. J. Biochem*. 262:211–217.
Lin, C.-L.G., L.A. Bristol, L. Jin, M. Dykes-Hoberg, T. Crawford, L. Clawson, and J.D. Rothstein. 1998. Aberrant RNA processing in a neurodegenerative disease: the cause of absent EAAT2, a glutamate transporter, in amyotrophic lateral sclerosis. *Neuron*. 20:589–602.
Martin, J.H., A.A. Mohit, and C.A. Miller. 1996. Developmental expression in the mouse nervous system of the $p49^{3F12}$ SAP kinase. *Mol. Brain Res.* 35:47–57.
Miller, K.E., and H.C. Joshi. 1996. Tubulin transport in neurons. *J. Cell Biol.* 133:1355–1366.
Miyasaka, H., S. Okabe, K. Ishiguro, T. Uchida, and N. Hirokawa. 1993. Interaction of the tail domain of high molecular weight subunits of neurofilaments with the COOH-terminal region of tubulin and its regulation by τ protein kinase II. *J. Biol. Chem*. 268:22695–22702.
Mohit, A.A., J.H. Martin, and C.A. Miller. 1995. $p49^{3F12}$ kinase: a novel MAP kinase expressed in a subset of neurones in the human nervous system. *Neuron*. 14:67–78.
Nikolic, M., H. Dudek, Y.T. Kwon, Y.F.M. Ramos, and L.H. Tsai. 1996. The cdk5/p35 kinase is essential for neurite outgrowth during neuronal differentiation. *Genes Dev*. 10:816–825.
Nixon, R.A. 1998. The slow axonal transport of cytoskeletal proteins. *Curr. Opin. Cell Biol.* 10:87–92.
Nixon, R.A., S.E. Lewis, M. Mercken, and R.K. Sihag. 1994a. Orthophosphate and methionine label separate pools of neurofilaments with markedly different axonal transport kinetics. *Neurochem. Res.* 19:1445–1453.
Nixon, R.A., P.A. Paskevich, R. Sihag, and C. Thayer. 1994b. Phosphorylation on carboxy terminus domains of neurofilament proteins in retinal ganglion cell neurons in vivo: influences on regional neurofilament spacing, and axon caliber. *J. Cell Biol.* 126:1031–1046.
Okabe, S., and N. Hirokawa. 1992. Differential behavior of photoactivated microtubules in growing axons of mouse and frog neurons. *J. Cell Biol.* 117: 105–120.
Okabe, S., and N. Hirokawa. 1993. Do photobleached fluorescent microtubules move?: re-evaluation of fluorescence laser photobleaching both in vitro and in growing *Xenopus* axon. *J. Cell Biol.* 120:1177–1186.
Okabe, S., H. Miyasaka, and N. Hirokawa. 1993. Dynamics of the neuronal intermediate filaments. *J. Cell Biol.* 121:375–386.
Reinsch, S.S., T.J. Mitchison, and M. Kirschner. 1991. Microtubule polymer assembly and transport during axonal elongation. *J. Cell Biol.* 115:365–376.
Rothstein, J.D. 1996. Excitotoxicity hypothesis. *Neurology*. 47:S19–S26.
Sabry, J., T.P. O'Connor, and M.W. Kirschner. 1995. Axonal transport of tubulin in Ti1 pioneer neurons in situ. *Neuron*. 14:1247–1256.
Schmidt, M.L., J.A. Martin, V.M.Y. Lee, and J.Q. Trojanowski. 1996. Convergence of Lewy bodies and neurofibrillary tangles in amygdala neurons of Alzheimer's disease and Lewy body disorders. *Acta. Neuropathol.* 91:475–481.
Schwarzschild, M.A., R.L. Cole, and S.E. Hyman. 1997. Glutamate, but not dopamine, stimulates stress-activated protein kinase and AP-1-mediated transcription in striatal neurons. *J. Neurosci.* 17:3455–3466.
Schwarzschild, M.A., R.L. Cole, M.A. Meyers, and S.E. Hyman. 1999. Contrasting calcium dependencies of SAPK and ERK activations by glutamate in cultured striatal neurons. *J. Neurochem*. 72:2248–2255.
Shaw, P.J. 1994. Excitotoxicity and motor neurone disease: a review of the evidence. *J. Neurol. Sci.* 124:6–13.
Shetty, K.T., W.T. Link, and H.C. Pant. 1993. cdc2-like kinase from rat spinal cord specifically phosphorylates KSPXK motifs in neurofilament proteins: isolation and characterization. *Proc. Natl. Acad. Sci. USA*. 90:6844–6848.
Sternberger, L.A., and N.H. Sternberger. 1983. Monoclonal antibodies distinguish phosphorylated and nonphosphorylated forms of neurofilaments. *Proc. Natl. Acad. Sci. USA*. 80:6126–6130.
Sun, D., C.L. Leung, and R.K.H. Liem. 1996. Phosphorylation of the high molecular weight neurofilament protein (NF-H) by cdk-5 and p35. *J. Biol. Chem*. 271:14245–14251.
Takeda, S., S. Okabe, T. Funakoshi, and N. Hirokawa. 1994. Differential dynamics of neurofilament-H protein and neurofilament-L protein in neurons. *J. Cell Biol.* 127:173–185.
Takeda, S., T. Funakoshi, and N. Hirokawa. 1995. Tubulin dynamics in neuronal axons of living zebrafish. *Neuron*. 14:1257–1264.
Terada, S., T. Nakarta, A.C. Peterson, and N. Hirokawa. 1996. Visualisation of slow axonal transport in vivo. *Science*. 273:784–788.
Trojanowski, J.Q., M.L. Schmidt, R.-W. Shin, G.T. Bramblett, D. Rao, and V.M. Lee. 1993. Altered tau and neurofilament proteins in neurodegenerarative diseases: diagnostic implications for Alzheimer's disease and Lewy body dementias. *Brain Pathol.* 3:45–54.
Trotti, D., A. Rolfs, N.C. Danbolt, R.H.J. Brown, and M.A. Hediger. 1999. SOD1 mutants linked to amyotrophic lateral sclerosis selectively inactivate a glial glutamate transporter. *Nat. Neurosci.* 2:427–433.
Veeranna, N.D. Amin, N.G. Ahn, H. Jaffe, C.A. Winters, P. Grant, and H.C. Pant. 1998. Mitogen-activated protein kinases (Erk1,2) phosphorylate Lys-Ser-Pro (KSP) repeats in neurofilament proteins NF-H and NF-M. *J. Neurosci.* 18:4008–4021.
Vickers, J.C., J.H. Morrison, V.L. Friedrich Jr., G.A. Elder, D.P. Perl, R.N. Katz, and R.A. Lazzarini. 1994. Age-associated and cell-type-specific neurofibrillary pathology in transgenic mice expressing the human midsized neurofilament subunit. *J. Neurosci.* 14:5603–5612.
Wang, L., C.-L. Ho, D. Sun, R.K.H. Liem, and A. Brown. 2000. Rapid movement of axonal neurofilaments interrupted by prolonged pauses. *Nat. Cell Biol.* 2:137–141.
Watson, D.F., J.W. Griffin, K.P. Fittro, and P.N. Hoffmann. 1989a. Phosphorylation-dependent immunoreactivity of neurofilaments increases during axonal maturation and beta-beta′-iminodipropionitrile intoxication. *J. Neurochem*. 53:1818–1829.
Watson, D.F., P.N. Hoffmann, K.P. Fittro, and J.W. Griffin. 1989b. Neurofilament and tubulin transport slows along the course of mature motor axons. *Brain Res.* 477:225–232.
Watson, D.F., K.P. Fittro, P.N. Hoffman, and J.W. Griffin. 1991. Phosphorylation-related immunoreactivity and the rate of transport of neurofilaments in chronic 2,5-hexanedione intoxication. *Brain Res.* 539:103–109.
Williamson, T.L., and D.W. Cleveland. 1999. Slowing of axonal transport is a very early event in the toxicity of ALS-linked SOD1 mutants to motor neurons. *Nat. Neurosci.* 2:50–56.
Wong, P.C., J. Marszalek, T.O. Crawford, Z.S. Xu, S.T. Hsieh, J.W. Griffin, and

D.W. Cleveland. 1995. Increasing neurofilament subunit NF-M expression reduces axonal NF-H, inhibits radial growth, and results in neurofilamentous accumulation in motor neurons. *J. Cell Biol.* 130:1413–1422.

Xia, Z.G., H. Dudek, C.K. Miranti, and M.E. Greenberg. 1996. Calcium influx via the NMDA receptor induces immediate-early gene-transcription by a MAP kinase/ERK-dependent mechanism. *J. Neurosci.* 16:5425–5436.

Yabe, J.T., A. Pimenta, and T.B. Shea. 1999. Kinesin-mediated transport of neurofilament protein oligomers in growing axons. *J. Cell Sci.* 112:3799–3814.

Yabe, J.T., C.W. Jung, W.K.H. Chan, and T.B. Shea. 2000. Phospho-dependent association of neurofilament proteins with kinesin in situ. *Cell Motil.Cytoskelet.* 45:249–262.

Yoon, M., R.D. Moir, V. Prahlad, and R.D. Goldman. 1998. Motile properties of vimentin intermediate filament networks in living cells. *J. Cell Biol.* 143: 147–157.

Yu, W., M.J. Schwei, and P.W. Baas. 1996. Microtubule transport and assembly during axon growth. *J. Cell Biol.* 1996:151–157.

Zhang, P., P. Tu, F. Abtahian, J.Q. Trojanowski, and V.M. Lee. 1997. Neurofilaments and orthograde transport are reduced in ventral root axons of transgenic mice that express human SOD1 with a G93A mutation. *J. Cell Biol.* 139:1307–1315.